Physical Properties of an Off-Center Impurity in the Tunneling Approximation. I. Statics*

M. GOMEZ, S. P. BOWEN,† AND J. A. KRUMHANSL
Laboratory of Atomic and Solid State Physics, Cornell University, Ithaca, New York
(Received 1 August 1966)

The present work presents the static properties of an off-center monopole impurity in a host lattice of octahedral symmetry. The energy levels of the lowest lying states were determined and classified for a model multi-well potential in the tunneling approximation. The effects of externally applied electric fields on the energy levels, specific heat, absorption spectrum, and induced dipole moment of the impurity are studied in detail for the model. The effects of uniaxial stress on the absorption spectrum are also studied.

I. INTRODUCTION

MANY experiments[1] suggest that substitutional Li^+ in KCl exhibits properties which are unexpected in view of the usual harmonic approximation for such impurities.[2]

Matthew,[3] calculating the potential acting on a Li^+ impurity in KCl, found unstable equilibrium positions at the lattice site and possible equilibrium sites away from the lattice site. Later work by Dienes *et al.*[4] confirmed this result. Both calculations indicate that the effective-force constant for the Li^+ at the lattice site is negative, and thus that harmonic approximations are not applicable to this problem. Hatcher and Wilson[5] have recently extended these potential calculations to several other point defects and host lattices. Since the usual harmonic approximation is not applicable to these impurities, it is necessary to have a theory which treats the problem satisfactorily.

The present paper presents a theory applicable to this type of impurity if the potential barriers between potential minima are large enough to justify a tunneling approximation.

The general treatment of the impurity problem begins with the separation of the terms in the full lattice-impurity Hamiltonian into three parts: the defect-lattice Hamiltonian H_L, the impurity Hamiltonian H_I,[6] and term H_C coupling H_L and H_I. Thus

$$H=H_L+H_I+H_C. \tag{1.1}$$

The defect-lattice Hamiltonian H_L is easily obtained by collecting all kinetic-energy terms of the host lattice and all terms of the potential in the small-oscillation approximation which are independent of the impurity. The terms H_I and H_C are derived from the impurity kinetic energy T_I and that part of the total potential energy V_{LI} which involves both the impurity and host coordinates. V_{LI} is expanded in the displacements of the host ions, but not with respect to the impurity coordinates. Thus the coefficients in this expansion are explicit functions of the impurity coordinate.

$$V_{LI}=V_{LI}^{(0)}(\{R(l,K)\},r_{\rm imp})+\sum_{l,K,\alpha}\times\frac{\partial V(\{R(l,K)\},r_{\rm imp})}{\partial R_\alpha(l,K)}u_\alpha(l,K). \tag{1.2}$$

Here, $\{R(l,K)\}$ indicates evaluation at the equilibrium positions of the host-lattice ions; $u_\alpha(l,K)$ is the αth component of the (l,K) host-lattice ion displacement.

The impurity Hamiltonian is

$$H_I=T_I+V_{LI}^{(0)}(\{R(l,K)\},r_{\rm imp}), \tag{1.3}$$

and $V_{LI}^{(0)}$ is the potential due to the static defect lattice. The coupling terms H_C to all desired orders are represented by the higher order terms in the expansion of V_{LI}.

The emphasis of this paper will be on the static aspects of the impurity problem and will involve calculations of the states and energies of H_I.

The eigenstates of H_I for the various possible potential wells are determined in the approximation of a linear combination of atomic orbitals (LCAO) for the lowest energy multiplet. A one-dimensional example will demonstrate the method.

II. TUNNELING MODEL

A. One-Dimensional Model

The model potential in which the impurity is assumed to move is the double-well potential

$$\begin{aligned} V&=V_A=\tfrac{1}{2}m\omega^2(x+x_0)^2 \quad \text{for} \quad x<0\\ &=V_B=\tfrac{1}{2}m\omega^2(x-x_0)^2 \quad \text{for} \quad x>0, \end{aligned} \tag{2.1}$$

* Supported by the U. S. Atomic Energy Commission under Contract No. AT(30-1)-3699, Technical Report No. (NYO-3699-1), and the Advanced Research Projects Agency.
† National Science Foundation Graduate Fellow.
[1] H. S. Sack and M. S. Moriarty, Solid State Commun. **3**, 936 (1965); G. Lombardo and R. O. Pohl, Phys. Rev. Letters **15**, 291 (1965); N. E. Byer and H. S. Sack, *ibid.* **17**, 72 (1966); F. Baumann, Bull. Am. Phys. Soc. **9**, 644 (1964); A. I. Lakatos and H. S. Sack, *ibid.* **11**, 229 (1966); H. Bogardus and H. S. Sack, *ibid.* **11**, 229 (1966).
[2] S. P. Bowen, M. Gomez, and J. A. Krumhansl, Phys. Rev. Letters **16**, 1105 (1966).
[3] J. A. D. Matthew, Materials Science Center Report No. 373, Cornell University, Ithaca, New York (unpublished).
[4] G. J. Dienes, R. D. Hatcher, R. Smoluchowski, and W. Wilson, Phys. Rev. Letters **16**, 25 (1966).
[5] R. D. Hatcher and W. Wilson (private communication).
[6] For simplicity, we consider only one impurity. Calculations including impurity-impurity interactions will be discussed elsewhere.

where m is the impurity mass. Linear combinations of the complete set of eigenfunctions a, a', a'', $\cdots$, which are solutions of the Schrödinger equation of a simple harmonic oscillator (SHO) whose center is displaced in the $-x$ direction a distance x_0 (i.e., potential V_A when the restriction $x<0$ is removed), and of the complete set b, b', b'', $\cdots$, which are solutions of the Schrödinger equation of a SHO whose center is displaced in the $+x$ direction a distance x_0, are sought as a solution to the problem. If the overlaps of the a and b wave functions are small enough, approximate solutions can be found for the two lowest levels of the system in terms of linear combinations of the ground-level wave functions a and b. Thus the problem is reduced to solving the secular equation

$$\begin{vmatrix} E_0-E & \eta-SE \\ \eta-SE & E_0-E \end{vmatrix}=0, \tag{2.2}$$

where

$$\begin{aligned} E_0&=\langle a|H|a\rangle=\langle b|H|b\rangle, \\ \eta&=\langle a|H|b\rangle, \\ S&=\langle a|b\rangle. \end{aligned} \tag{2.3}$$

Its solution gives two roots which are the energies of the two lowest states of the system; these are

$$\begin{aligned} E_+&=(E_0+\eta)/(1+S), \\ E_-&=(E_0-\eta)/(1-S). \end{aligned} \tag{2.4}$$

These two roots are associated with two sets of simultaneous equations whose solutions give the proper admixture of the a and b wave functions for the wave functions of the two lowest levels of the system. The normalized wave functions are

$$\begin{aligned} \psi_+&=(a+b)/[2(1+S)]^{1/2} \\ &\qquad\text{(corresponds to energy } E_+), \\ \psi_-&=(a-b)/[2(1-S)]^{1/2} \\ &\qquad\text{(corresponds to energy } E_-). \end{aligned} \tag{2.5}$$

The wave functions a and b can be written explicitly as

$$\begin{aligned} a&=c\,\exp[(-m\omega/2\hbar)(x+x_0)^2], \\ b&=c\,\exp[(-m\omega/2\hbar)(x-x_0)^2], \end{aligned} \tag{2.6}$$

where c is the normalization factor; thus the overlap integral is

$$S=\langle a|b\rangle=\exp[-(m\omega/\hbar)x_0^2]; \tag{2.7}$$

E_0 and η are

$$\begin{aligned} E_0&=\langle a|H|a\rangle_A+\langle a|H|a\rangle_B, \\ \eta&=\langle a|H|b\rangle_A+\langle a|H|b\rangle_B, \end{aligned} \tag{2.8}$$

where the subscripts of the brackets specify the region over which the integral is carried out, i.e., $\langle\ |\ |\ \rangle_A$ indicates that the integral must be carried over the region $x<0$; $\langle\ |\ |\ \rangle_B$, over the region $x>0$; and $\langle\ |\ |\ \rangle_\infty$, over all available space. The above expressions are simplified by using the following relationships:

$$\begin{aligned} \langle a|H|a\rangle&=\langle a|T+V_A|a\rangle_\infty-\langle a|V_B-V_A|a\rangle_B \\ &=\tfrac{1}{2}\hbar\omega-\langle a|V_B-V_A|a\rangle_B, \end{aligned} \tag{2.9}$$

$$\begin{aligned} \langle a|H|b\rangle&=\langle a|T+V_A|b\rangle_\infty-\langle a|V_B-V_A|b\rangle_B \\ &=\textstyle\sum_{a'}\langle a|T+V_A|a'\rangle_\infty\langle a'|b\rangle_\infty-\langle a|V_B-V_A|b\rangle_B \\ &=\tfrac{1}{2}\hbar\omega S-\langle a|V_B-V_A|b\rangle_B, \end{aligned} \tag{2.10}$$

where $\sum_{a'}$ indicates a sum over the complete set of wave functions, a, a', a'', $\cdots$. In obtaining the above relationships, use has been made of the fact that the a's form a complete and orthogonal set of eigenfunctions of the SHO with Hamiltonian $H=T+V_A$. Substituting the results obtained above into E_0 and η, the following expressions for the energies of the system are obtained:

$$\begin{aligned} E_+&=\tfrac{1}{2}\hbar\omega+(\langle a|V_B-V_A|a\rangle_B \\ &\qquad+\langle a|V_B-V_A|b\rangle_B)/(1+S), \\ E_-&=\tfrac{1}{2}\hbar\omega+(\langle a|V_B-V_A|a\rangle_B \\ &\qquad-\langle a|V_B-V_A|b\rangle_B)/(1-S). \end{aligned} \tag{2.11}$$

The two integrals involved in this expression can be easily evaluated.

$$\begin{aligned} E_0'&=\langle a|V_B-V_A|a\rangle_B \\ &=-Kc^2\{\exp[-(m\omega/\hbar)x_0^2]/2(m\omega/\hbar) \\ &\quad-x_0(\tfrac{1}{2}[\pi\hbar/m\omega]^{1/2})(1-\Phi([m\omega/\hbar]^{1/2}x_0))\}, \end{aligned} \tag{2.12}$$

$$\begin{aligned} \eta'&=\langle a|V_B-V_A|b\rangle_B=-Kc^2 \\ &\qquad\times\exp[-(m\omega/\hbar)x_0^2]/2(m\omega/\hbar). \end{aligned} \tag{2.13}$$

Here, $K=2m\omega^2x_0$ (from $V_B-V_A=-Kx$ for $x>0$) and $\Phi([m\omega/\hbar]x_0)$ is the error integral.

For small S (i.e., $S<0.05$), an asymptotic expansion for the error integral can be used;

$$\begin{aligned} &1-\Phi[(m\omega/\hbar]^{1/2}x_0) \\ &\qquad\simeq\exp[-(m\omega/\hbar)x_0^2]/(\pi m\omega/\hbar)^{1/2}x_0, \end{aligned} \tag{2.14}$$

and

$$\begin{aligned} E_0'&=Q_0S, \\ \eta'&=QS, \end{aligned} \tag{2.15}$$

where

$$S=\exp[-(m\omega/\hbar)x_0^2].$$

Q_0 and Q are only weakly dependent on the position of the well minima. The strong exponential dependence of the matrix elements on the position of the well minima has been factored out in the form of overlap integrals. In Appendix II it is shown that this factorization can also be carried out in three dimensions.

From Eqs. (2.13) and (2.14), if the tunneling approximation is valid (i.e., for small S), $Q_0\ll Q$ and thus $E_0'\ll\eta'$. Neglecting E_0' compared with η' and S compared with unity, Eqs. (2.11) simplify to

$$\begin{aligned} E_+&=\tfrac{1}{2}\hbar\omega+\eta', \\ E_-&=\tfrac{1}{2}\hbar\omega-\eta'. \end{aligned} \tag{2.16}$$

B. Three-Dimensional Model

For the cubic symmetry of the impurity's environment, there are three multi-well potentials which are consistent with the octahedral symmetry. These are XY_6 with 6 minima in the [100] directions, XY_8 with 8 minima in the [111] directions, and XY_{12} with 12 minima in the [110] directions. See Fig. 1.

The model for each of these three cases begins with a tractable potential described by certain parameters: frequency ω and well locations $\mathbf{r}_0$. These model parameters may be determined either by comparison with experiment or by adjusting the parameters to approximate a theoretical potential calculated from first principles. For the calculation of the low-lying states (i.e., those whose energies are below the theoretical barrier heights), the model potential can be adjusted to the theoretical one by letting them have the same minima position and the same curvature at the bottom of the wells. The above fitting will yield correct results as long as their respective barriers have comparable opacity (where opacity is used here in the same spirit that it is used in the WKB approximation). But if the above method does not yield comparable opacities, as is the case in the Matthew's potential (see Fig. 2), the conditions of equal curvature at the well minima must be sacrificed in order to achieve comparable opacities of the barriers. Figure 2 illustrates the results of the two methods of fitting the theoretical potential.

The model potential for each case XY_n ($n=6$, 8, 12) is the appropriate three-dimensional analog of the one-dimensional double-well harmonic oscillator [Eq. (2.1)]. As in Eq. (2.1), to write down these potentials, it is necessary to specify the potentials in several different regions and match the potentials together at the boundaries. The XY_8 case yields a simple expression for the model potential if each displaced harmonic-oscillator potential is characterized by only one frequency (i.e., is isotropic).

$$V=\tfrac{1}{2}m\omega^2[(|x|-x_0)^2+(|y|-x_0)^2+(|z|-x_0)^2]. \quad (2.17)$$

A priori, of course, there is no reason to suppose that the off-center wells should be isotropic or even to require that they should have inversion symmetry about

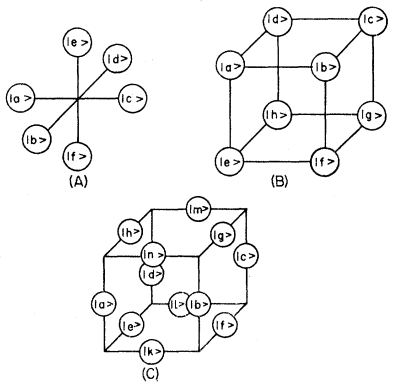

FIG. 1. Location of well minima and labeling of the localized harmonic-oscillator (HO) basis states for (A) XY_6, (B) XY_8, (C) XY_{12}.

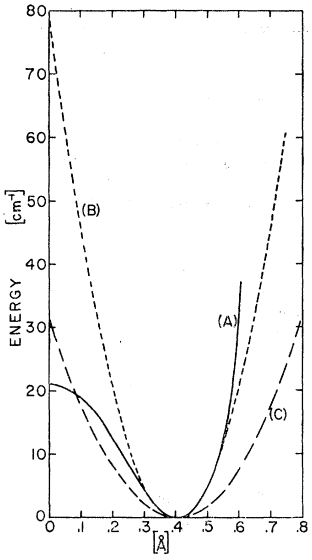

FIG. 2. Two possible ways for fitting the HO multi-well potential to a potential calculated from first principles. (A) Potential calculated from first principles by Matthew (Ref. 3) for Li:KCl in the [100] direction. (B) Model potential adjusted so that the wells will have the same minima position and the same curvature at the bottom of the wells. (C) Model potential adjusted so that the wells will have the same minima position and their respective barriers the same opacity, where opacity is used here in the same spirit that it is used in the WKB approximation.

their minimum positions. Nonisotropic wells have been studied in the form of ellipsoids of revolution consistent with O_h symmetry for XY_6 and XY_8, as well as for XY_{12}, although for XY_{12} a general ellipsoid will satisfy the symmetry conditions. Some of the ellipsoidal well's properties are discussed in Appendix II.

The energy levels of the lowest lying multiplet are found from the correct linear combinations of basis states. For these ground-state splittings, the basis states are normalized SHO ground-state wave functions[7] centered at each well minimum. The labeling of the basis states for the XY_8, XY_6, and XY_{12} models are shown in Fig. 1. The explicit form of basis state $|a\rangle$ in the XY_8 model is

$$|a\rangle=(m\omega/\pi\hbar)^{3/4}\exp\{-(m\omega/2\hbar) \times[(x-x_0)^2+(y-x_0)^2+(z-x_0)^2]\}. \quad (2.18)$$

The correct linear combinations of basis states for each of these three models are easily determined by group-theoretical methods. The wave functions for each irreducible representation were used to evaluate the energies of that eigenstate. The results of this evaluation are shown in Table I for XY_8 and in Appendix I for XY_6 and XY_{12}.

An interesting physical significance can be associated with the overlap integrals $\{S\}$ and the tunnel-splitting matrix elements. For XY_8, for instance, the overlap integrals S, S', and S'', and the tunnel-splitting matrix elements η, μ, and ν are characterized by the location of the two basis states in each matrix element. S and η represent overlap and tunneling along the cube edges. S' and μ represent overlap and tunneling across the cube

[7] The admixture of higher excited states can be taken into account by doing a perturbation calculation if necessary, but their contribution can be shown to be negligible as long as $\hbar\omega$ is greater than the tunneling splittings.

TABLE I. XY_8 energies and wave functions.

$$\psi(A_{1g})=[8(1+3S+3S'+S'')]^{-1/2}(a+b+c+d+e+f+g+h),$$
$$\psi_x(T_{1u})=[8(1+S-S'-S'')]^{-1/2}[(a+b+e+f)-(d+c+g+h)],$$
$$\psi_y(T_{1u})=[8(1+S-S'-S'')]^{-1/2}[(b+c+f+g)-(a+d+e+h)],$$
$$\psi_z(T_{1u})=[8(1+S-S'-S'')]^{-1/2}[(a+b+c+d)-(e+f+g+h)],$$
$$\psi_{yz}(T_{2g})=[8(1-S-S'+S'')]^{-1/2}[(b+c+e+h)-(a+d+f+g)],$$
$$\psi_{xz}(T_{2g})=[8(1-S-S'+S'')]^{-1/2}[(a+b+g+h)-(c+d+e+f)],$$
$$\psi_{xy}(T_{2g})=[8(1-S-S'+S'')]^{-1/2}[(b+d+f+h)-(a+c+g+e)],$$
$$\psi(A_{2u})=[8(1-3S+3S'-S'')]^{-1/2}[(b+d+e+g)-(a+c+f+h)];$$
$$E(A_{1g})=(E_0+3\eta+3\mu+\nu)/(1+3S+3S'+S''),$$
$$E(T_{1u})=(E_0+\eta-\mu-\nu)/(1+S-S'-S''),$$
$$E(T_{2g})=(E_0-\eta-\mu+\nu)/(1-S-S'+S''),$$
$$E(A_{2u})=(E_0-3\eta+3\mu-\nu)/(1-3S+3S'-S''),$$

where a, b, c, d, e, f, g, and h are the localized basis states pictured in Fig. 1, and

$$S=\langle a|b\rangle=\langle b|c\rangle=\cdots,$$
$$S'=\langle a|f\rangle=\langle a|h\rangle=\cdots,$$
$$S''=\langle a|g\rangle=\langle b|h\rangle=\cdots,$$
$$E_0=\langle a|H|a\rangle=\langle b|H|b\rangle=\cdots,$$
$$\eta=\langle a|H|b\rangle=\langle b|H|c\rangle=\cdots,$$
$$\mu=\langle a|H|c\rangle=\langle a|H|h\rangle=\cdots,$$
$$\nu=\langle a|H|g\rangle=\langle b|H|h\rangle=\cdots,$$

where H is the impurity Hamiltonian.

faces. S'' and ν represent overlap and tunneling through the cube along a body diagonal.

In Appendix II, it is shown that E_0, η, μ, and ν can be written, in a form analogous to the one-dimensional case, in terms of new parameters E_0', η', μ', and ν'. In terms of these new parameters, the energy-level expressions for XY_8 become

$$E(A_{1g})=\tfrac{1}{2}\hbar\omega+(E_0'+3\eta'+3\mu'+\nu')/(1+3S+3S'+S''),$$
$$E(T_{1u})=\tfrac{1}{2}\hbar\omega+(E_0'+\eta'-\mu'-\nu')/(1+S-S'-S''),$$
$$E(T_{2g})=\tfrac{1}{2}\hbar\omega+(E_0'-\eta'-\mu'+\nu')/(1-S-S'+S''),$$
$$E(A_{2u})=\tfrac{1}{2}\hbar\omega+(E_0'-3\eta'+3\mu'-\nu')/(1-3S+3S'-S''). \quad (2.19)$$

The relative magnitudes of these matrix elements η', μ', and ν' depend quite strongly upon the well separation. As will be shown in Appendix II, for our choice of basis states, this dependence is through a factor of the form $\exp[-(m\omega/\hbar)x_0^2]$, where $2x_0$ is the separation distance between two adjacent well minima. This strong dependence on the relative position of the wells makes S and η' dominant for isotropic wells. This implies that the orbitals have their maximum amplitude along the line joining adjacent well minima. Thus the ion may be thought of semiclassically as shuttling around the surface of the cube for XY_8 and XY_{12} (or along the edges of a rhombohedron for XY_6), rather than tunneling through the center as would be appropriate if ν' for XY_6 and XY_8, and σ' for XY_{12} were dominant. This kind of motion is equivalent to a quasirotational motion associated with rigid rotators in an octahedral field with large barriers (see Fig. 8). The lowest level structure of the Devonshire[8] molecular-rotor model coincidentally resembles the present results.

It must be pointed out that the dominance of S and η' which imparts a rotational nature to the impurity tunnel-split spectrum is valid even for ellipsoidal wells, as long as the ratio of the two frequencies describing the harmonic potentials is less than five. But, clearly, as discussed in Appendix II, for sufficiently elliptical wells, ν' becomes dominant and the tunnel-split spectrum becomes identical to that associated with a translational kind of motion.

[8] A. F. Devonshire, Proc. Roy. Soc. (London) **A153**, 601 (1936).

III. ELECTRIC-FIELD EFFECTS

The Hamiltonian for the model impurity under the influence of an electric field will be

$$H'=T+V+eE_{\text{loc}}(\alpha x+\beta y+\gamma z), \quad (3.1)$$

where V is the multi-well potential, E_{loc} is the field seen by the impurity (not the externally applied field), e is the charge of the impurity, and α, β, γ are the direction cosines of the field with respect to the x, y, and z axes. We will assume that the wave functions of the tunnel-split levels (see Appendix I) provide us with an approximate complete set to construct the solutions for the perturbed Hamiltonian H'. Thus the problem is reduced to the solution of a relatively small secular equation.[9]

The matrix elements entering the secular equation will be (i) the diagonal matrix elements that will be of the form

$$\langle\psi(\Gamma)|H'|\psi(\Gamma)\rangle=\langle\psi(\Gamma)|T+V|\psi(\Gamma)\rangle=E(\Gamma), \quad (3.2)$$

where $\psi(\Gamma)$ is the eigenfunction of one of the ground-state multiplet states and $E(\Gamma)$ is its associated energy; (ii) the nonzero off-diagonal matrix elements that will be of the form

$$\langle\psi(\Gamma_u)|H'|\psi(\Gamma_g)\rangle=\langle\psi(\Gamma_u)|eE_{\text{loc}}(\alpha x+\beta y+\gamma z)|\psi(\Gamma_g)\rangle$$
$$=ex_0E_{\text{loc}}(\alpha N_1+\beta N_2+\gamma N_3)+O[S^2], \quad (3.3)$$

where $\psi(\Gamma_u)$ and $\psi(\Gamma_g)$ are odd-parity and even-parity states, respectively, x_0 is the position of the well's minima, and N_1, N_2, and N_3 are constants which depend on the wave function. Notice that, to second order in the overlap integral, the off-diagonal matrix elements are independent of the actual shape of the potential wells (i.e., independent of the ω's) and depend only on the position of the well minima. This result will be valid for both elliptical and spherical potentials as long as each potential well is symmetric with respect to inversion about its minimum position and as long as the tunneling approximation is valid.

[9] It should be pointed out that this approximation will yield good results as long as the matrix elements between the first-excited-state multiplet and the ground-state multiplet wave functions are smaller than the energy difference between the multiplets. This approximation does not impose an upper limit to the region where the ground-state multiplet has levels increasing in energy as the electric field increases. Upon taking the first-excited-state multiplet into account, it is found that for sufficiently high fields the levels of the ground-state multiplet that increase in energy with increasing field are forced down by levels from the first-excited-state multiplet with the appropriate symmetry.

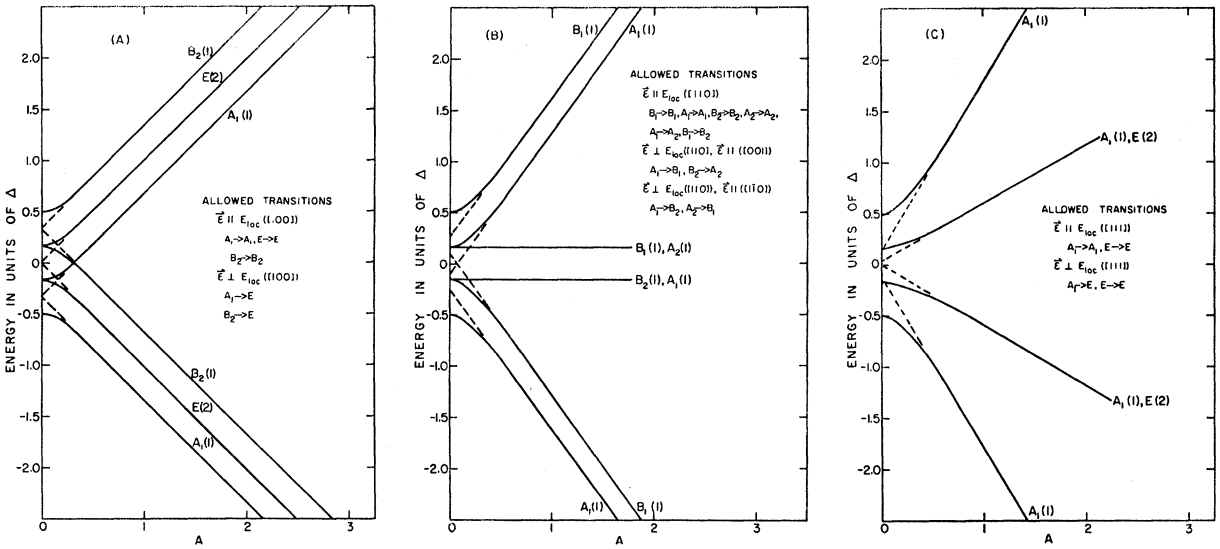

FIG. 3. Electric-field splittings for XY_8 when η is the dominant tunneling parameter, with the corresponding dipole-allowed transitions and the energy in units of Δ. (A) Field applied in the [100] direction. (B) Field applied in the [110] direction. (C) Field applied in the [111] direction.

With the wave functions in Appendix I, the secular equations appropriate to each one of the three cases are obtained. The secular equation for XY_8 then becomes

$$\begin{vmatrix} n_1-E/\Delta & \gamma A & \beta A & \alpha A & 0 & 0 & 0 & 0 \\ \gamma A & n_2-E/\Delta & 0 & 0 & 0 & \alpha A & \beta A & 0 \\ \beta A & 0 & n_2-E/\Delta & 0 & \alpha A & 0 & \gamma A & 0 \\ \alpha A & 0 & 0 & n_2-E/\Delta & \beta A & \gamma A & 0 & 0 \\ 0 & 0 & \alpha A & \beta A & n_3-E/\Delta & 0 & 0 & \gamma A \\ 0 & \alpha A & 0 & \gamma A & 0 & n_3-E/\Delta & 0 & \beta A \\ 0 & \beta A & \gamma A & 0 & 0 & 0 & n_3-E/\Delta & \alpha A \\ 0 & 0 & 0 & 0 & \gamma A & \beta A & \alpha A & n_4-E/\Delta \end{vmatrix} = 0, \qquad (3.4)$$

where

$$n_1=E(A_{1g})/\Delta\,,\ n_2=E(T_{1u})/\Delta\,,\ n_3=E(T_{2g})/\Delta\,,$$
$$n_3=E(A_{2u})/\Delta\,,\ A=eE_{\rm loc}x_0/\Delta\,,$$
$$\text{and}\quad \Delta=E(A_{2u})-E(A_{1g})\,.$$

Thus the value of each matrix element is expressed in units of the energy difference between maximum and minimum energies in the multiplet.

The dimensionless quantities n_1, n_2, n_3, and n_4 contain all the pertinent information on the nature of the tunnelings, since they are determined by the relative magnitudes of the energy terms η', μ', ν', and σ' through Eq. (2.19). The effect that the different types of tunneling have on the electric-field properties can be studied by changing the relative magnitudes of the energy terms η', μ', ν', and σ'.

The secular equation was solved and the energy eigenvalues and eigenvectors were obtained as a function of A and as a function of the direction cosines of the electric field (see Figs. 3 and 11). Electric fields parallel to ⟨100⟩, ⟨110⟩, and ⟨111⟩ (which reduce the O_h symmetry to C_{4v}, C_{2v}, and C_{3v}, respectively) were considered.

From the reduced symmetry group, the splittings of levels and the electric-dipole selection rules can be easily obtained. Figure 3 and Appendix III show the nature of the splitting and the selection rules for a few of the cases that were studied. As can be observed in Fig. 3, there is a fine structure due to tunneling superimposed on the usual Stark effect. At high field (i.e., $A\gg1$), this structure becomes independent of the field and depends only on the tunneling parameters; in particular, for XY_8 when the electric field is applied in the [100] direction, the fine structure is determined by the parameter η' even in the case where the zero-field tunnel splitting is dominated by ν'. Physically, this can be understood as follows: When the energy associated with the electric field exceeds the tunneling energy it will effectively localize the particle in planes (a,b,c,d) and (e,f,g,h), thus freezing out the tunneling through the center but still allowing the impurity to tunnel freely

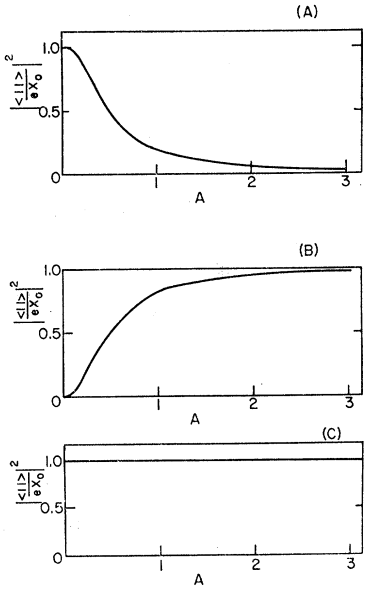

FIG. 4. The square of the dipole-transition matrix elements in units of ex_0 for the XY_8, η-dominant, and $E_{\rm loc}\|[100]$ system of Fig. 3(A). (A) For transition $A_1 \rightarrow A_1$, $E \rightarrow E$, and $B_2 \rightarrow B_2$. (B) For transitions of the form $A_1 \rightarrow E$ and $B_2 \rightarrow E$ which are forbidden in the absence of an electric-field perturbation. (C) For transitions of the form $A_1 \rightarrow E$ and $B_2 \rightarrow E$ which are allowed even in the absence of a field.

in the planes perpendicular to the field. In general, it is to be expected, then, that the fine structure of the levels in the strong-field limit should be independent of the tunnelings that the field freezes out and should depend only on the tunnelings that take place in planes perpendicular to the field.

The squares of the off-diagonal matrix elements for the dipole operator were calculated and classified into three different types: (i) those that represent allowed dipole transitions for $E_{\rm loc}=0$ with the electromagnetic field $\mathcal{E}$ parallel to the static applied field $E_{\rm loc}$ [this will progressively weaken as the applied field is increased; see Fig. 4(A)]; (ii) those that represent allowed dipole transitions with $\mathcal{E} \perp E_{\rm loc}$ [these will be independent of the magnitude of $E_{\rm loc}$; see Fig. 4(C)]; (iii) those that represent transitions which are forbidden for $E_{\rm loc}=0$ [these will increase as $E_{\rm loc}$ increases; see Fig. 4(B)]. As can be seen from Fig. 4, the sum of the square of the off-diagonal matrix elements for the dipole operator is independent of the perturbing field, as required by the theorem of spectroscopic stability.[10]

The electric field will induce a quantum-mechanical dipole moment on the system. In particular, each state of the multiplet will have an induced dipole moment associated with it given by

$$\langle p\rangle_i = \langle \psi_i | e\mathbf{r} | \psi_i \rangle , \tag{3.5}$$

where the ψ_i are the wave functions obtained from the secular equation (3.4). The functional dependence of the dipole moments $\langle p\rangle_i$ on the electric field $E_{\rm loc}$ is shown in Fig. 5. For small A (i.e., $ex_0E_{\rm loc}<\Delta$), $\langle p\rangle_i$ is proportional to A, while for $A\gg 1$, $\langle p\rangle_i$ saturates and the expectation values of the distance from the lattice site (i.e., $\langle p\rangle_i/e$) are a measure of the perpendicular distance from the plane in which the particle is now localized to the center of the cube.

The $\langle p\rangle_i$ obey the following simple sum rule:

$$\sum_{i=1}^{N} \langle p\rangle_i = 0 , \tag{3.6}$$

where N is the number of wave functions in the ground-state multiplet. The thermal average of the system's dipole moment will be

$$\langle p\rangle^T = \Big(\sum_{i=1}^{N} \langle p\rangle_i e^{-\beta E_i}\Big) \Big/ \Big(\sum_{i=1}^{N} e^{-\beta E_i}\Big) , \tag{3.7}$$

where E_i is an eigenvalue of Eq. (3.4) associated with wave function ψ_i and $\beta = 1/kT$. From the sum rule it follows for the case $\beta E_i \ll 1$ (for all i) that the net dipole of the system will be proportional to $1/T$. This result is analogous to the classical result at high temperatures when the field is unable to align the dipole associated with the displacement of the particle. For the other extreme case, when $\beta E_{i\neq 1} \gg \beta E_1$,

$$\langle p\rangle^T = \langle p\rangle_1 , \tag{3.8}$$

where "1" refers to the lowest energy state in the multiplet. Thus, contrary to the classical case, $\langle p\rangle^T$ becomes temperature-independent, showing the usual discrepancy between classical and QM systems at low temperatures.

For the strong-field limit $A\gg 1$, the $E_i \propto A$ and the Boltzmann factor is dominated by the electric-field energy, while for weak fields the Boltzmann factor is

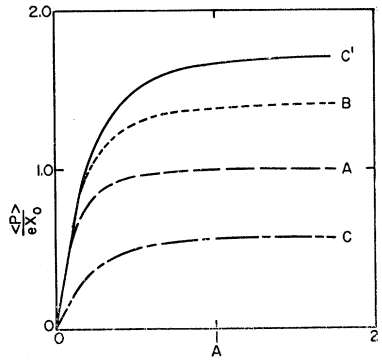

FIG. 5. The absolute value of the induced dipole moments associated with the states of the multiplet, in units of ex_0, as a function of the electric field, for the XY_8 system with the tunneling parameter $\eta \gg \mu, \nu$. (A) $E_{\rm loc}\|[100]$, for all states. (B) $E_{\rm loc}\|[110]$, for states that are split by the field. (C) $E_{\rm loc}\|[111]$, for states that show relatively weak splitting with respect to the field. (C') $E_{\rm loc}\|[111]$, for states that show relatively strong splitting with respect to the field.

[10] J. H. Van Vleck, *Theory of Electric and Magnetic Susceptibilities* (Oxford University Press, New York, 1952), pp. 137–139.

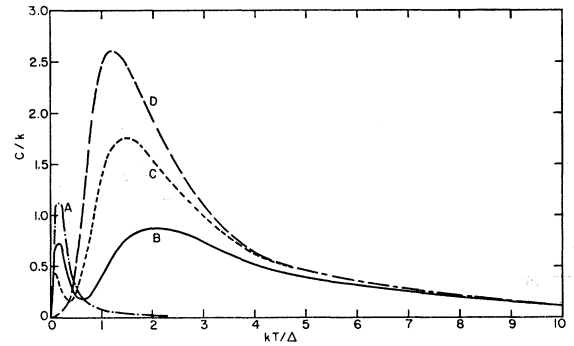

FIG. 6. The specific heat C of the XY_8 under the influence of an electric field in units of k (Boltzmann's constant), as a function of kT/Δ. For the following electric fields $[A=E_{\rm loc}(ex_0)/\Delta]$: (A) $A=0.0$; (B) $A=2.5$ in the [100] direction; (C) $A=2.5$ in the [110] direction; (D) $A=2.5$ in the [111] direction.

dominated by the tunneling-energy parameters. Nevertheless, because of the dependence of the $\langle p\rangle_i$'s on $E_{\rm loc}$, at high temperature both the strong- and weak-field limits go as $E_{\rm loc}/T$ (see Appendix III for the details of the $\langle p\rangle^T$'s for the different cases).

IV. SPECIFIC HEAT

The low-lying levels into which the ground level of the system is split by the tunneling will give rise to a Schottky anomaly in the system's specific heat. Since this anomalous specific heat will be proportional to the number of impurities in the crystal and its maximum value will occur when kT is of the order of δ (the average energy spacing between levels in the multiplet), the observability of the anomaly will depend on the relative magnitude of the anomalous specific heat for a given impurity concentration and the lattice T^3 specific heat at temperature $kT=\delta$. The effect that an electric field has on the specific-heat anomaly is shown in Fig. 6. The appearance of two peaks in the specific heat when the field is in the [100] and [110] directions is due to the tunneling fine structure that is superimposed on the Stark splitting (see Fig. 3). The increase in the maximum of the specific heat as the field goes from the [100] to the [111] direction is due mainly to the term

$$E_{\rm loc}d\langle p\rangle^T/dT \tag{4.1}$$

associated with the dipole energy.

V. STRESS FIELD

The application of a uniaxial stress to this type of impurity provides a useful tool for probing its structure. From group-theoretic methods, the splittings and allowed electric dipole transitions can be deduced for special symmetries. These results are presented for XY_8 in Fig. 7 and for XY_6 in Appendix IV.

A convenient way to summarize the response of this model to uniaxial stress is to calculate the change in the first moment of the absorption spectrum for a transition between two levels ϵ_a and ϵ_b. In general, either or both of the levels may be degenerate in the absence of the stress, and degenerate perturbation theory must be considered. Let $|\Phi_i\rangle$ be the degenerate states for ϵ_a and $|\Phi_i'\rangle$ the perturbed states; similarly, $|\psi_i\rangle$ unperturbed and $|\psi_i'\rangle$ perturbed for the ϵ_b level. The first moment in the presence of a stress is obtained using the following function[11]:

$$f(\epsilon)=\sum_{ij} Z^{-1}e^{-\beta\epsilon_a'}\langle\Phi_i'|D|\psi_j'\rangle\langle\psi_j'|D|\Phi_i'\rangle\delta(\epsilon_b'-\epsilon_a'-\epsilon)\,, \tag{5.1}$$

where D is the dipole operator and the sum is restricted to the two levels under consideration. The first moment $\langle\epsilon\rangle$ is

$$\langle\epsilon\rangle=\frac{1}{A}\int d\epsilon\, f(\epsilon)\epsilon\,, \tag{5.2}$$

where

$$A=\int d\epsilon\, f(\epsilon)\,.$$

If the impurity is acted upon by a stress perturbation H', then the change of the energies in first-order–degenerate perturbation theory will be $\langle\psi_i'|H'|\psi_i'\rangle=\Delta\epsilon_i$. If $\Delta\epsilon_i<\epsilon_a$, then an expression for the change in the first moment of the absorption due to the perturbation can be written as a temperature-independent factor $\langle\Delta\epsilon'\rangle$ times a Boltzmann factor.

$$\langle\Delta\epsilon\rangle=\frac{e^{-\beta\epsilon_a{}^0}}{z}\langle\Delta\epsilon'\rangle=\frac{e^{-\beta\epsilon_a{}^0}}{z}\Big(\frac{1}{A}\sum_{ij}\langle\Phi_i'|D|\psi_j'\rangle$$

$$\times\langle\psi_j'|D|\Phi_i'\rangle[\langle\psi_j'|H'|\psi_j'\rangle-\langle\Phi_i'|H'|\Phi_i'\rangle]\Big). \tag{5.3}$$

The temperature-independent shift $\langle\Delta\epsilon'\rangle$ can be calculated in first-order–degenerate perturbation theory in terms of the unperturbed states $|\Phi_i\rangle$ and $|\psi_j\rangle$ if unitary transformations U and V can be found so that

$$|\Phi_i'\rangle=\sum_j V_{ji}|\Phi_j\rangle\,,$$
$$|\psi_i'\rangle=\sum_j U_{ji}|\psi_j\rangle\,. \tag{5.4}$$

For uniaxial stress applied in an arbitrary direction, a determination of U and V requires a solution of the usual eigenvalue problem associated with degenerate perturbation theory. However, for certain special symmetry axes it is possible to determine the U and V matrices from symmetry considerations alone.

The expression for $\langle\Delta\epsilon'\rangle$ in terms of the U and V

[11] C. H. Henry, S. E. Schnatterly, and C. P. Slichter, Phys. Rev. Letters **13**, 130 (1964).

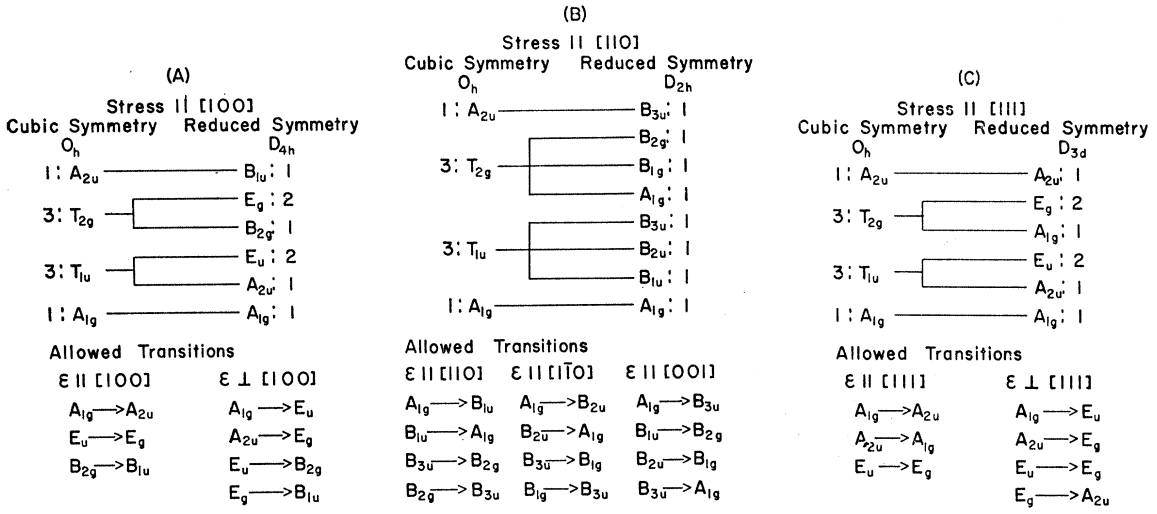

FIG. 7. Group-theoretic classification and allowed electric-dipole transitions for the stress-induced splittings of the XY_8 system with the stress in the following directions: (A) stress ∥[100], (B) stress ∥[110], (C) stress ∥[111].

matrices is

$$\langle\Delta\epsilon'\rangle=\frac{1}{A}\sum_{imlnpq}V_{mi}V_{ni}^{*}V_{qi}V_{pi}^{*}\langle\psi_l|D|\Phi_m\rangle\times\langle\Phi_n|D^{\dagger}|\psi_l\rangle\langle\Phi_p|H'|\Phi_q\rangle-\frac{1}{A}\sum_{ilmnpq}U_{mi}U_{ni}^{*}U_{qi}U_{pi}^{*}\langle\Phi_l|D^{\dagger}|\psi_m\rangle\times\langle\psi_n|D|\Phi_l\rangle\langle\psi_p|H'|\psi_q\rangle. \quad (5.5)$$

The further reduction of the terms in Eq. (5.5) proceeds from an examination of the symmetry properties of the stress Hamiltonian H'.

The stress Hamiltonian can be written for an arbitrary uniaxial stress $-P_{lk}$ in terms of irreducible representations Γ^{ν} of the O_h group. Thus

$$H'=\sum_{\mu\nu}h_{\mu}(\Gamma^{\nu})e_{\mu}(\Gamma^{\nu}). \quad (5.6)$$

The factors $h_{\mu}(\Gamma^{\nu})$ are linear combinations of first derivatives of the potential coupling the impurity to the host lattice with the appropriate symmetry. These factors are tabulated in Appendix IV. If α, β, and γ are the direction cosines of the uniaxial stress $-P_{lk}$ with respect to the cube's principal axes, then the factors $e_{\mu}(\Gamma^{\nu})$ may be written

$$\begin{aligned}
e(A_{1g})&=-(S_{11}+2S_{12})P,\\
e_1(E_g)&=-(2\gamma^2-\alpha^2-\beta^2)(S_{11}-S_{12})P,\\
e_2(E_g)&=-(\alpha^2-\beta^2)(S_{11}-S_{12})P,\\
e_1(T_{2g})&=-S_{44}\beta\gamma P,\\
e_2(T_{2g})&=-S_{44}\alpha\gamma P,\\
e_3(T_{2g})&=-S_{44}\alpha\beta P,
\end{aligned} \quad (5.7)$$

where $-P$ is the magnitude of the stress, e.g., $-P_{xy}=-\alpha\beta P$, and S_{11}, S_{12}, and S_{44} are stiffness coefficients of the lattice adjacent to the impurity.

The expansion of H' in terms of definite irreducible representations of the O_h group allows a reduction of Eq. (5.5) to a similar expansion, since the product space of $|\Phi_p\rangle\cdot|\Phi_q\rangle$ can be expanded in elements of each of the same irreducible representations. The simplification arises from the well-known symmetry selection rule that $\langle\psi(\Gamma_1)|h(\Gamma_2)|\psi(\Gamma_3)\rangle$ vanishes unless Γ_2 is contained in $\Gamma_1\times\Gamma_3$. These considerations give rise to an expansion of $\langle\Phi_p|H'|\Phi_q\rangle$ in terms of the irreducible elements of O_h.

$$\langle\Phi_p|H'|\Phi_q\rangle=\sum_{\mu\nu}H_{\mu}(\Gamma^{\nu})(a_{\mu}(\Gamma^{\nu}))_{pq}. \quad (5.8)$$

Here the factors $H_{\mu}(\Gamma^{\nu})$ are properly symmetrized linear combinations of matrix elements of $h_{\mu}(\Gamma^{\nu})$ multiplied by the appropriate $e_{\mu}(\Gamma^{\nu})$, and the $a_{\mu}(\Gamma^{\nu})$ are constant matrices. For reference, the $H_{\mu}(\Gamma^{\nu})$ and the $a_{\mu}(\Gamma^{\nu})$ are tabulated in Appendix IV for the T_{1u} state. An expansion of $\langle\Delta\epsilon'\rangle$ in terms of the irreducible representations of O_h is accomplished by substituting Eq. (5.8) into Eq. (5.5).

$$\langle\Delta\epsilon'\rangle=\frac{1}{A^{(a)}}\sum_{\mu\nu}H_{\mu}^{(a)}(\Gamma^{\nu})K_{\mu}^{(a)}(\Gamma^{\nu})-\frac{1}{A^{(b)}}\sum_{\mu\nu}H_{\mu}^{(b)}(\Gamma^{\nu})K_{\mu}^{(b)}(\Gamma^{\nu}), \quad (5.9)$$

where

$$K_{\mu}^{(a)}(\Gamma^{\nu})=\sum_{i}(V^{\dagger}D^{\dagger}DV)_{ii}(V^{\dagger}a_{\mu}^{(a)}(\Gamma^{\nu})V)_{ii},$$

and

$$K_{\mu}^{(b)}(\Gamma^{\nu})=\sum_{i}(U^{\dagger}DD^{\dagger}U)_{ii}(U^{\dagger}a_{\mu}^{(b)}(\Gamma^{\nu})U)_{ii}.$$

Here (a) and (b) denote the two levels being considered and D is that submatrix of the dipole matrix which connects the Φ and ψ states.

For all of the levels of this model, the $H_\mu^{(a)}(\Gamma^\nu)$ can be reduced to

$$\begin{aligned} &H(A_{1g})=A(a)e(A_{1g}),\\ &H_1(E_g)=B_1(a)e_1(E_g),\\ &H_2(E_g)=B_2(a)e_2(E_g),\\ &H_i(T_{2g})=C_i(a)e_i(T_{2g}),\quad i=1,\,2,\,3 \end{aligned} \tag{5.10}$$

where A, B_1, B_2, and C_i refer to certain matrix elements of $\langle\psi(\Gamma)|h(\Gamma')|\psi(\Gamma)\rangle$. A major result of this section will be to quote the specific matrix elements for the allowed transitions of the ground-state tunneling multiplets and their order of magnitude.

The shift $\langle\Delta\epsilon'\rangle$ is directly calculable from the tunneling model if the V and U matrices are known. It must be emphasized again that these matrices can only be determined with the help of symmetry alone in special directions: [100], [110], and [111]. To obtain these matrices for arbitrary directions, the secular equation of degenerate perturbation theory must be solved.[12] In quoting the results for the special symmetry directions, it is convenient to quote the slope $-\partial\Delta\epsilon'/\partial P$. For the $A_{1g}\rightarrow T_{1u}$ transition,

[100] stress: $\alpha=1,\ \beta=0,\ \gamma=0$

$$-\partial\epsilon/\partial P=A(S_{11}+2S_{12})+B_1(2\alpha'^2-\gamma'^2-\beta'^2)(S_{11}-S_{12}),$$

[010] stress: $\alpha=0,\ \beta=1,\ \gamma=0$

$$-\partial\epsilon/\partial P=A(S_{11}+2S_{12})+B_1(2\beta'^2-\alpha'^2-\gamma'^2)(S_{11}-S_{12}),$$

[001] stress: $\alpha=0,\ \beta=0,\ \gamma=1$

$$-\partial\epsilon/\partial P=A(S_{11}+2S_{12})+B_1(2\gamma'^2-\alpha'^2-\beta'^2)(S_{11}-S_{12}),$$

[110] stress: $\alpha=\beta=1/\sqrt{2},\ \gamma=0$

$$-\partial\epsilon/\partial P=A(S_{11}+2S_{12})-\tfrac{1}{2}B_1(2\gamma'^2-\alpha'^2-\beta'^2)(S_{11}-S_{12})+C\alpha'\beta'S_{44},$$

[101] stress: $\alpha=1/\sqrt{2},\ \beta=0,\ \gamma=1/\sqrt{2}$

$$-\partial\epsilon/\partial P=A(S_{11}+2S_{12})-\tfrac{1}{2}B_1(2\beta'^2-\alpha'^2-\gamma'^2)(S_{11}-S_{12})+C\alpha'\gamma'S_{44},$$

[011] stress: $\alpha=0,\ \beta=\gamma=1/\sqrt{2}$

$$-\partial\epsilon/\partial P=A(S_{11}+2S_{12})-\tfrac{1}{2}B_1(2\alpha'^2-\beta'^2-\gamma'^2)(S_{11}-S_{12})+C\beta'\gamma'S_{44},$$

[111] stress: $\alpha=\beta=\gamma=1/\sqrt{3}$

$$-\partial\epsilon/\partial P=A(S_{11}+2S_{12})+\tfrac{2}{3}CS_{44}(\alpha'\beta'+\beta'\gamma'+\alpha'\gamma'),$$

(5.11)

and

$$\begin{aligned} A&=A(T_{1u})-A(A_{1g})=\langle\psi_z(T_{1u})|h(A_{1g})|\psi_z(T_{1u})\rangle-\langle\psi(A_{1g})|h(A_{1g})|\psi(A_{1g})\rangle,\\ B_1&=B_1(T_{1u})=\langle\psi_z(T_{1u})|h_1(E_g)|\psi_z(T_{1u})\rangle,\\ C&=C(T_{1u})=\langle\psi_x(T_{1u})|h_3(T_{2g})|\psi_y(T_{1u})\rangle, \end{aligned}$$

where α', β', and γ' are the direction cosines of the electromagnetic polarization vector with respect to the principal axes of the cube. All of the other transitions, with exceptions to be noted in Appendix IV, yield the same expressions for the slope $-\partial\epsilon/\partial P$, but with different values for the coefficients A, B, and C. The explicit equations for the coefficients A, B, and C are quoted in Appendix IV. The various coefficients A, B, and C can be calculated explicitly from the model if the interaction between the host lattice and the impurity is known.

For the tunneling model which has been discussed in this paper, the coefficients $[A(\Gamma_1)-A(\Gamma_2)]$, B, and C can be shown to be of order S $[O(S)]$, where S is the overlap integral between the localized basis states.

It is relatively easy to see why $A(\Gamma_1)-A(\Gamma_2)$ is $O(S)$; for example, for XY_8, the $A_{1g}\rightarrow T_{1u}$ transition is

$$\begin{aligned} A(A_{1g})&=\langle\psi(A_{1g})|h(A_{1g})|\psi(A_{1g})\rangle=\tfrac{1}{8}[\langle a|h(A_{1g})|a\rangle+\cdots+\langle h|h(A_{1g})|h\rangle]+O(S),\\ A(T_{1u})&=\langle\psi_x(T_{1u})|h(A_{1g})|\psi_x(T_{1u})\rangle=\tfrac{1}{8}[\langle a|h(A_{1g})|a\rangle+\cdots+\langle h|h(A_{1g})|h\rangle]+O(S). \end{aligned} \tag{5.12}$$

Thus $A(T_{1u})-A(A_{1g})=O(S)$. The same argument carries through for the other transitions.

Either of the B coefficients can be written as

$$\begin{aligned} B=(1/24)[&\langle a|h_2(E_g)|a\rangle+\langle b|h_2(E_g)|b\rangle+\langle c|h_2(E_g)|c\rangle+\langle d|h_2(E_g)|d\rangle+\langle e|h_2(E_g)|e\rangle\\ &+\langle f|h_2(E_g)|f\rangle+\langle g|h_2(E_g)|g\rangle+\langle h|h_2(E_g)|h\rangle]+O(S). \end{aligned} \tag{5.13}$$

[12] This point is not emphasized in a treatment of this stress problem in another context by W. Gebhardt and K. Maier [Phys. Status Solidi 8, 303 (1965)]. That the dependence of $\langle\Delta\epsilon'\rangle$ on α, β, and γ for arbitrary stress directions is quite complicated, away from the "special" directions, can be easily seen by solving the secular equation for the E_g levels of the XY_6 model, a very tractable problem.

Now consider a rotation U_z by $\frac{1}{2}\pi$ about the z axis, such that $a\rightarrow b\rightarrow c\rightarrow d\rightarrow a$, $e\rightarrow f\rightarrow g\rightarrow h\rightarrow e$. For this transformation,

$$Uh_2(E_g)U^\dagger=-h_2(E_g). \tag{5.14}$$

Then, for example,

$$\langle a|h_2(E_g)|a\rangle=\langle Ua|Uh_2(E_g)U^\dagger|Ua\rangle=-\langle b|h_2(E_g)|b\rangle, \tag{5.15}$$

and the leading terms in B vanish pairwise, so that $B=O(S)$.

A similar argument shows that the C coefficients are also $O(S)$. For example, consider $C(T_{1u})$ of XY_8;

$$C=\langle\psi_x(T_{1u})|h_3(T_{2g})|\psi_y(T_{1u})\rangle=\tfrac{1}{8}[\langle b|h_3(T_{2g})|b\rangle+\langle f|h_3(T_{2g})|f\rangle+\langle h|h_3(T_{2g})|h\rangle+\langle d|h_3(T_{2g})|d\rangle$$
$$-\langle a|h_3(T_{2g})|a\rangle-\langle g|h_3(T_{2g})|g\rangle-\langle e|h_3(T_{2g})|e\rangle-\langle c|h_3(T_{2g})|c\rangle]+O(S). \tag{5.16}$$

Considering the same rotation as in the previous argument we note that now $Uh_3(\Gamma_{2g})U^\dagger=h_3(T_{2g})$ and thus

$$\langle a|h_3(T_{2g})|a\rangle=\langle Ua|Uh_3(\Gamma_{2g})U^\dagger|Ua\rangle$$
$$=\langle b|h_3(T_{2g})|b\rangle, \tag{5.17}$$

and similarly for the other terms. Thus $C(T_{1u})=O(S)$. An identical argument may be applied to the other C's.

For such tunneling models, the response of the first moment of the absorption is $O(S)$. This means that for an impurity in which the potential is determined by Coulomb interactions, polarization effects, dipole-dipole interactions, and repulsive interactions with its neighbors, the response of the system to uniaxial stress will be relatively small.

While the response of this impurity to electric fields depends only upon x_0 (to first order in S), the stress response depends on ω and x_0 and is much more sensitive to the precise values of the well parameters. Because of this, numerical values of A, B, and C for some physical model will not be given here.

VI. CONCLUSIONS

The tunneling multi-well model discussed in the text as an appropriate model for describing the physical properties of an off-center impurity has the following features:

(i) The ground state in the absence of tunneling splits into a multiplet when tunneling is allowed. The general features of this multiplet are quite independent of the shape of the wells, while the relative values of the energy spacings between levels depends strongly on the relative values of the energy barriers between wells.

(ii) When an electric-field perturbation is applied to the impurity, a Stark-type splitting of the multiplet will result with a fine structure superimposed on it. Only the "fine structure" will reflect the tunneling structure.

(iii) The thermal average of the system's dipole moment will be proportional to $E_{\rm loc}(ex_0)/\Delta$ for weak fields [i.e., $(A=E_{\rm loc}(ex_0)/\Delta)\ll 1$] and will saturate for strong fields (i.e., $A\gg 1$).

(iv) The specific heat of the tunneling system under the influence of an electric field will show a multilevel Schottky anomaly with up to two maxima in its structure.

(v) The first nonzero term in the stress-induced splitting will be proportional to the overlap integral S. Thus the effect of stress on the tunneling system will be relatively weak, since S is a small number for a tunneling system.

ACKNOWLEDGMENTS

It is a pleasure to acknowledge discussions with Professor H. Sack, Professor R. Pohl, and Professor A. J. Sievers. We also wish to thank Mrs. K. Lakatos for invaluable aid in bringing this work to fruition.

APPENDIX I: ENERGIES AND WAVE FUNCTIONS FOR XY_6 AND XY_{12}

The location of the well minima and localized basis states for XY_6 is shown in Fig. 1(A). The wave functions and energies for this model are listed below.

XY_6 Wave Functions and Energies

$$\psi(A_{1g})=[6(1+4S+S')]^{-1/2}(a+b+c+d+e+f),$$
$$\psi_x(T_{1u})=[2(1-S')]^{-1/2}(a-c),$$
$$\psi_y(T_{1u})=[2(1-S')]^{-1/2}(b-d),$$
$$\psi_z(T_{1u})=[2(1-S')]^{-1/2}(e-f),$$
$$\psi_1(E_g)=[12(1-2S+S')]^{-1/2}[a+b+c+d-2(e+f)],$$
$$\psi_2(E_g)=[4(1-2S+S')]^{-1/2}(a-b+c-d),$$
$$E(A_{1g})=(E_0+4\eta+\mu)/(1+4S+S'),$$
$$E(T_{1u})=(E_0-\mu)/(1-S'),$$
$$E(E_g)=(E_0-2\eta+\mu)/(1-2S+S'),$$

where

$$E_0=\langle a|H|a\rangle=\langle b|H|b\rangle=\cdots,$$
$$\eta=\langle a|H|b\rangle=\langle a|H|d\rangle=\cdots,$$
$$\mu=\langle a|H|c\rangle=\langle e|H|f\rangle=\cdots,$$
$$S=\langle a|b\rangle=\langle b|c\rangle=\cdots,$$
$$S'=\langle a|c\rangle=\langle b|d\rangle=\cdots.$$

The location and labeling of the localized basis states for the XY_{12} model is shown in Fig. 1(C). The wave functions and energies are listed below.

XY_{12} Wave Functions and Energies

$$\psi(A_{1g})=[12(1+4S+2S'+4S''+S''')]^{-1/2}(a+b+c+d+e+f+g+h+k+l+m+n),$$
$$\psi_1(E_g)=[24(1-2S+2S'-2S''+S''')]^{-1/2}[a+b+c+d+n+k+l+m-2(e+f+g+h)],$$
$$\psi_2(E_g)=[8(1-2S+2S'-2S''+S''')]^{-1/2}[(a+b+c+d)-(n+k+l+m)],$$
$$\psi_1(T_{1u})=[8(1+2S-2S''-S''')]^{-1/2}[(a+b+k+n)-(c+d+l+m)],$$
$$\psi_2(T_{1u})=[8(1+2S-2S''-S''')]^{-1/2}[(a+d+e+h)-(b+c+f+g)],$$
$$\psi_3(T_{1u})=[8(1+2S-2S''-S''')]^{-1/2}[(g+h+m+n)-(e+f+k+l)],$$
$$\psi_1(T_{2g})=[4(1-2S'+S''')]^{-1/2}(a+c-b-d),$$
$$\psi_2(T_{2g})=[4(1-2S'+S''')]^{-1/2}(h+f-e-g),$$
$$\psi_3(T_{2g})=[4(1-2S'+S''')]^{-1/2}(n+l-m-k),$$
$$\psi_1(T_{2u})=[8(1-2S+2S''-S''')]^{-1/2}[(e+f+n+m)-(h+g+k+l)],$$
$$\psi_2(T_{2u})=[8(1-2S+2S''-S''')]^{-1/2}[(b+c+e+h)-(d+a+g+f)],$$
$$\psi_3(T_{2u})=[8(1-2S+2S''-S''')]^{-1/2}[(c+d+n+k)-(b+a+m+l)],$$
$$E(A_{1g})=(E_0+4\eta+2\mu+4\nu+\sigma)/(1+4S+2S'+4S''+S'''),$$
$$E(E_g)=(E_0-2\eta+2\mu-2\nu+\sigma)/(1-2S+2S'-2S''+S'''),$$
$$E(T_{1u})=(E_0+2\eta-2\nu-\sigma)/(1+2S-2S''-S'''),$$
$$E(T_{2g})=(E_0-2\mu+\sigma)/(1-2S'+S'''),$$
$$E(T_{2u})=(E_0-2\eta+2\nu-\sigma)/(1-2S+2S''-S'''),$$

where

$$E_0=\langle a|H|a\rangle=\langle b|H|b\rangle=\cdots,$$
$$\eta=\langle a|H|n\rangle=\langle a|H|k\rangle=\cdots,$$
$$\mu=\langle a|H|b\rangle=\langle a|H|d\rangle=\cdots,$$
$$\nu=\langle a|H|g\rangle=\langle a|H|f\rangle=\cdots,$$
$$\sigma=\langle a|H|c\rangle=\langle b|H|d\rangle=\cdots,$$
$$S=\langle a|n\rangle=\langle a|k\rangle=\cdots,$$
$$S'=\langle a|b\rangle=\langle a|d\rangle=\cdots,$$
$$S''=\langle a|g\rangle=\langle a|f\rangle=\cdots,$$
$$S'''=\langle a|c\rangle=\langle b|d\rangle=\cdots.$$

APPENDIX II: APPROXIMATE EXPRESSIONS OF THE TUNNELING MULTIPLET ENERGIES FOR SPECIAL CASES

The parameters entering the expressions for the energies in XY_8 have the explicit form[13]

$$E_0=\langle a|H|a\rangle_\infty=\sum_N\langle a|T+V_N|a\rangle_N=\langle a|T+V_A|a\rangle_\infty+\sum_N{}'\langle a|V_N-V_A|a\rangle_N$$
$$\simeq\tfrac{1}{2}\hbar\omega+3\langle a|V_B-V_A|a\rangle_B+O(S^2)\simeq\tfrac{1}{2}\hbar\omega+3E_0',$$
$$\eta=\langle a|H|b\rangle_\infty=\sum_N\langle a|T+V_N|b\rangle_N=(\sum_{a'}\langle a|T+V_A|a'\rangle_\infty\langle a'|b\rangle_\infty+\sum_{N'}\langle a|V_N-V_A|b\rangle_N)$$
$$\simeq\tfrac{1}{2}\hbar\omega S+\langle a|V_B-V_A|b\rangle_B+O(S^2)\simeq\tfrac{1}{2}\hbar\omega S+\eta',$$
$$\mu=\langle a|H|c\rangle_\infty=\sum_N\langle a|T+V_N|c\rangle_N=(\sum_{a'}\langle a|T+V_A|a'\rangle_\infty\langle a'|c\rangle_\infty+\sum_{N'}\langle a|V_N-V_A|c\rangle_N)$$
$$\simeq\tfrac{1}{2}\hbar\omega S'+\langle a|V_C-V_A|c\rangle_C+O(S^3)\simeq\tfrac{1}{2}\hbar\omega S'+\mu',$$
$$\nu=\langle a|H|g\rangle_\infty=\sum_N\langle a|T+V_N|g\rangle=(\sum_{a'}\langle a|T+V_A|a'\rangle_\infty\langle a'|g\rangle_\infty+\sum_{N'}\langle a|V_N-V_A|g\rangle_N$$
$$\simeq\tfrac{1}{2}\hbar\omega S''+\langle a|V_G-V_A|g\rangle_G+O(S^4)\simeq\tfrac{1}{2}\hbar\omega S''+\nu', \quad \text{(A2.1)}$$

[13] The subscript N on the matrix elements $\langle a|H|a\rangle_N$ denotes a limitation on the range of integration to that region associated with the localized well n. This is the three-dimensional generalization of the notation in Eqs. (2.8), (2.9), and (2.10).

where $\sum_{a'}$ indicates the sum over the complete set of wave functions, $a, a', a'', \cdots$, and $\sum_{N'}$ indicates the sum over all wells except well V_A and where only the two largest matrix elements in the above expressions have been kept. The terms neglected are at least of order S^2.

The parameters η', μ', and ν' are always negative quantities. They can always be expressed in terms of the overlap integrals, in a fashion similar to the one-dimensional case, as

$$\begin{aligned} E_0' &= Q_0 S, \\ \eta' &= QS, \\ \mu' &= Q'S', \\ \nu' &= Q''S'', \end{aligned} \tag{A2.2}$$

where

$$S=\langle a|b\rangle,\ S'=\langle a|c\rangle,\quad \text{and}\quad S''=\langle a|g\rangle.$$

For spherical wells, we have

$$S'=S^2,\ S''=S^3,\ Q_0\simeq 0.1Q,\ Q'\lesssim Q,\ Q''<Q.$$

For the tunneling approximation to be valid, $S<0.1$; thus

$$\eta'\gg\mu'\gg\nu'.$$

The expression for the four energy levels reduces to

$$\begin{aligned} E(A_{1g}) &= \tfrac{1}{2}\hbar\omega - 3|\eta'|, \\ E(T_{1u}) &= \tfrac{1}{2}\hbar\omega - |\eta'|, \\ E(T_{2g}) &= \tfrac{1}{2}\omega + |\eta'|, \\ E(A_{2u}) &= \tfrac{1}{2}\hbar\omega + 3|\eta'|, \end{aligned} \tag{A2.3}$$

while for potentials which are ellipsoids of revolution with their semimajor axis oriented along the radial direction and a ratio of maximum frequency to minimum frequency of $\omega/\omega_1\simeq 40$, we have

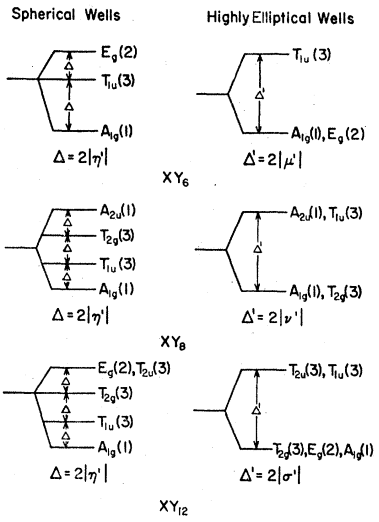

FIG. 8. Ground-state tunnel split multiplet, both in the spherical and highly elliptical well limit. For the XY_6, XY_6, and XY_{12} models.

$$S''\gg S\gg S',\ Q_0\simeq 0.1Q,\ Q''>Q\gtrsim Q',$$

and thus $\nu'\gg\eta'\gg\mu'$, making the expression for the energy levels reduce to

$$\begin{aligned} E(A_{1g}) &= \tfrac{1}{6}\hbar(\omega_1+2\omega) - |\nu'|, \\ E(T_{1u}) &= \tfrac{1}{6}\hbar(\omega_1+2\omega) + |\nu'|, \\ E(T_{2g}) &= \tfrac{1}{6}\hbar(\omega_1+2\omega) - |\nu'|, \\ E(A_{2u}) &= \tfrac{1}{6}\hbar(\omega_1+2\omega) + |\nu'|. \end{aligned} \tag{A2.4}$$

It is worth mentioning that, although at some point between the two extreme limits of highly ellipsoidal and spherical wells (actually $\omega/\omega_1\simeq 7$) $\nu'\simeq\eta'$, μ' always re-

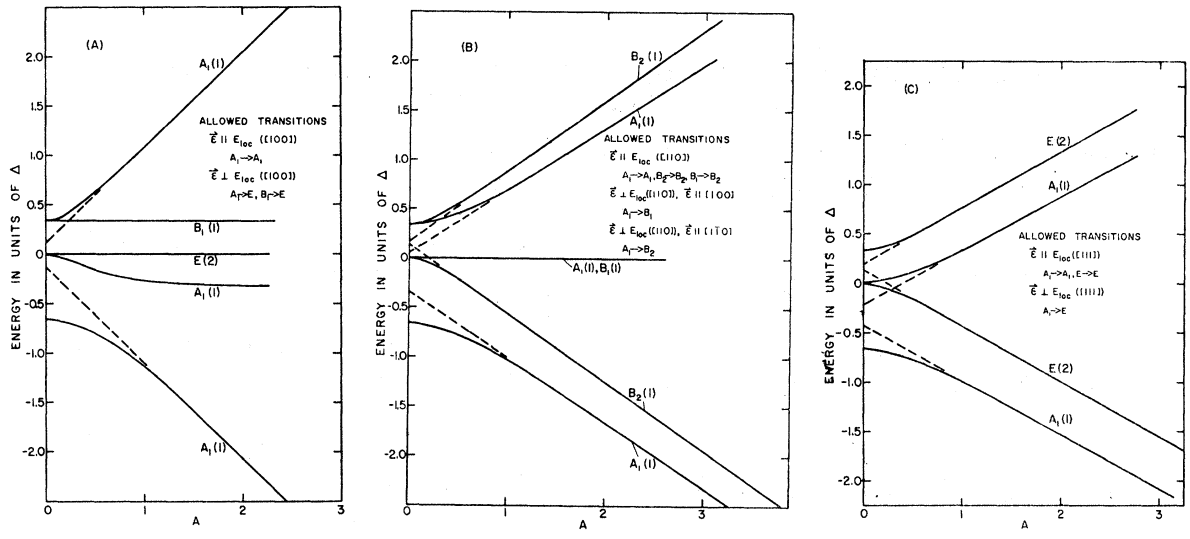

FIG. 9. Electric-field splittings for XY_6, when η is the dominant tunneling parameter, with the corresponding allowed dipole transitions and the energy in units of Δ. (A) Field applied in the [100] direction. (B) Field applied in the [110] direction. (C) Field applied in the [111] direction.

mains smaller than η' and never helps shape the energy configuration.

The models XY_6 and XY_{12} yield similar results and we will only quote them.

For spherical wells XY_6,

$$S'=S^2,\ Q_0\simeq 0.1Q,\ Q\gtrsim Q',$$

where $S=\langle a|b\rangle$, $S'=\langle a|c\rangle$, $E_0'=Q_0=Q_0S$, $\eta'=QS$, and $\mu'=Q'S'$. Therefore, $\eta'\gg\mu'$ and the expressions for the energies become

$$\begin{aligned} E(A_{1g})&=\tfrac{1}{2}\hbar\omega-4|\eta'|,\\ E(T_{1u})&=\tfrac{1}{2}\hbar\omega,\\ E(E_g)&=\tfrac{1}{2}\hbar\omega+2|\eta'|, \end{aligned} \tag{A2.5}$$

while for highly ellipsoidal wells we get

$$S'\gg S,\ Q_0\simeq 0.1Q,\ Q'\gtrsim Q,$$

so that $\mu'\gg\eta'$ and the energies become

$$\begin{aligned} E(A_{1g})&=\tfrac{1}{2}\hbar(\omega_1+2\omega)-|\mu'|,\\ E(T_{1u})&=\tfrac{1}{2}\hbar(\omega_1+2\omega)+|\mu'|,\\ E(E_g)&=\tfrac{1}{2}\hbar(\omega_1+2\omega)-|\mu'|. \end{aligned} \tag{A2.6}$$

For spherical wells XY_{12} we have

$$S'=S^2,\ S''=S^3,\ S'''=S^4,$$
$$Q_0\simeq 0.1Q,\ Q\gtrsim Q',\ Q>Q'',\ Q>Q''',$$

where

$$S=\langle a|n\rangle,\ S'=\langle a|d\rangle,\ S''=\langle a|g\rangle,\ S'''=\langle a|c\rangle,$$
$$E_0=Q_0S,\ \eta'=QS,\ \mu'=Q'S',\ \nu'=Q''S'',\ \sigma'=Q'''S'''.$$

Therefore $\eta'\gg\mu'\gg\nu'\gg\sigma'$ and the expressions for the energies become

$$\begin{aligned} E(A_{1g})&=\tfrac{1}{2}\hbar\omega-4|\eta'|,\\ E(T_{1u})&=\tfrac{1}{2}\hbar\omega-2|\eta'|,\\ E(T_{2g})&=\tfrac{1}{2}\hbar\omega,\\ E(E_g)&=\tfrac{1}{2}\hbar\omega+2|\eta'|,\\ E(T_{2u})&=\tfrac{1}{2}\hbar\omega+2|\eta'|, \end{aligned} \tag{A2.7}$$

while for highly ellipsoidal wells we get

$$S'''\gg S\gg S'\gg S'',\ Q_0\simeq 0.1Q,\ Q'''>Q,Q'',Q'.$$

Thus $\sigma'\gg\eta'\gg\mu'\gg\nu'$ and the energies become

$$\begin{aligned} E(A_{1g})&=\tfrac{1}{6}\hbar(\omega_1+2\omega)-|\sigma'|,\\ E(T_{1u})&=\tfrac{1}{6}\hbar(\omega_1+2\omega)+|\sigma'|,\\ E(T_{2g})&=\tfrac{1}{6}\hbar(\omega_1+2\omega)-|\sigma'|,\\ E(E_g)&=\tfrac{1}{6}\hbar(\omega_1+2\omega)-|\sigma'|,\\ E(T_{2u})&=\tfrac{1}{6}\hbar(\omega_1+2\omega)+|\sigma'|. \end{aligned} \tag{A2.8}$$

See Fig. 8 for the different types of tunneling multiplets discussed here.

APPENDIX III: ELECTRIC FIELD

The field splittings can be calculated for XY_6 in the same manner that they were calculated for XY_8 from the following secular equation:

$$0=\begin{vmatrix} n_1-E/\Delta & \alpha A/\sqrt{3} & \beta A/\sqrt{3} & \gamma A/\sqrt{3} & 0 & 0\\ \alpha A/\sqrt{3} & n_2-E/\Delta & 0 & 0 & \alpha A/\sqrt{6} & \alpha A/\sqrt{2}\\ \beta A/\sqrt{3} & 0 & n_2-E/\Delta & 0 & \beta A/\sqrt{6} & -\beta A/\sqrt{2}\\ \gamma A/\sqrt{3} & 0 & 0 & n_2-E/\Delta & -2\gamma A/\sqrt{6} & 0\\ 0 & \alpha A/\sqrt{6} & \beta A/\sqrt{6} & -2\gamma A/\sqrt{6} & n_3-E/\Delta & 0\\ 0 & \alpha A/\sqrt{2} & -\beta A/\sqrt{2} & 0 & 0 & n_3-E/\Delta \end{vmatrix}, \tag{A3.1}$$

where

$$n_1=E(A_{1g})/\Delta,\ n_2=E(T_{1u})/\Delta,$$
$$n_3=E(E_g)/\Delta,\ \Delta=E(E_g)-E(A_{1g}),$$

and all other symbols have the same meaning as in Eq. (3.3). Figure 9 shows, for XY_6, the resulting field splitting when the field is in each one of the three symmetry directions, and the corresponding dipole selection rules. Figures 10 and 11 show the effect that different values of the n's (i.e., different relative values of the tunneling parameter) have on the field splitting for the XY_6, XY_8 systems. As can be seen from the figures, at high fields (i.e., in the region where the splitting depends linearly on the field) the Stark effect is independent of the n's, while the superimposed fine structure depends on the n's.

The thermal average of the dipole moment $\langle p\rangle^T$ for the three symmetry directions of the electric field is shown in Figs. 12 and 13 as a function of the applied field with $kT=\Delta$. As discussed in Sec. III, $\langle p\rangle^T$ is proportional to E_{loc} in the weak-field region and saturates at strong fields to a value which is dependent only on the geometry of the well minima. Table II gives the appropriate geometric factors for XY_6 and XY_8.

Since, as can be seen from Figs. 14 and 15, $\langle p\rangle^T$ is independent of the n's (i.e., independent of the tunneling parameters) in the regions of weak and strong fields, it

TABLE II. Values of $\langle p\rangle^T/ex_0$ at saturation for XY_6 and XY_8.

Field direction	[100]	[110]	[111]
XY_6	1	$1/\sqrt{2}$	$1/\sqrt{3}$
XY_8	1	$\sqrt{2}$	$\sqrt{3}$

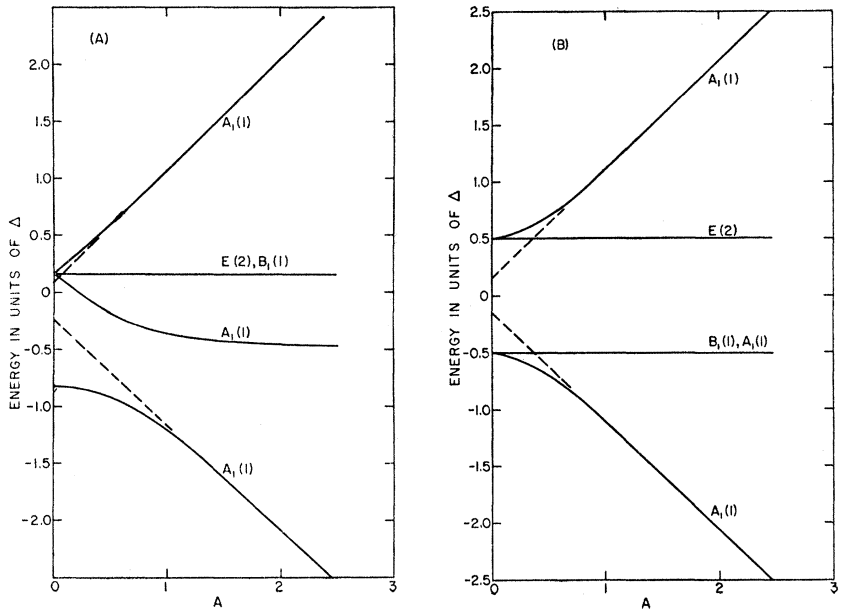

FIG. 10. Electric-field splittings for XY_6 with the applied field in the [100] direction and the energy in units of Δ for the following relative values of the tunneling parameters: (A) $\eta=\mu$; (B) $\mu\gg\eta$. For the splittings when $\eta\gg\mu$, see Fig. 9(A).

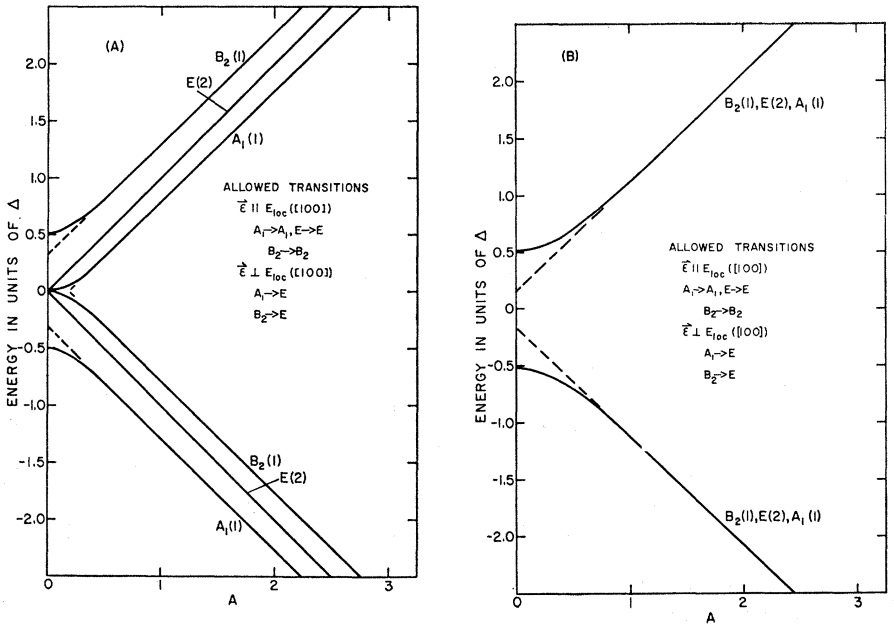

FIG. 11. Electric-field splittings for XY_8 with the applied field in the [100] direction and the energy in units of Δ for the following realtive values of the tunneling parameters: (A) $\eta=\nu\gg\mu$; (B) $\nu\gg\eta,\mu$. For the splittings when $\eta\gg\mu,\nu$, see Fig. 3(A).

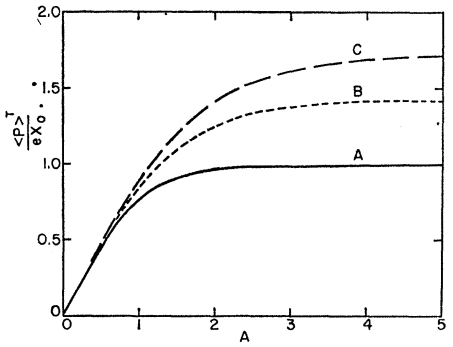

FIG. 12. Thermal average of the XY_8 system's dipole moment $\langle p\rangle^T$ in units of ex_0 with the tunneling parameter $\eta\gg\mu,\nu$, for a temperature $kT=\Delta$ (where k is Boltzmann's constant) as a function of the applied field. (A) Field in the [100] direction. (B) Field in the [110] direction. (C) Field in the [111] direction.

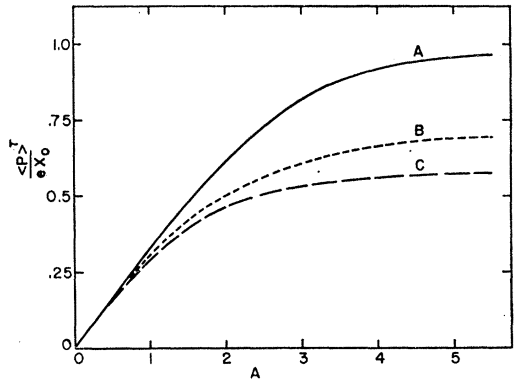

FIG. 13. Thermal average of the XY_6 system's dipole moment $\langle p\rangle^T$ in units of ex_0 with the tunneling parameter $\eta\gg\mu$, for a temperature $kT=\Delta$ (where k is Boltzmann's constant) as a function of the applied field. (A) Field in the [100] direction. (B) Field in the [110] direction. (C) Field in the [111] direction.

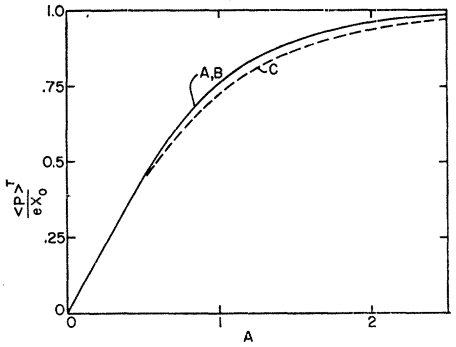

FIG. 14. Thermal average of the XY_8 system's dipole moment $\langle p\rangle^T$ in units of ex_0 as a function of a field applied in the [100] direction, at a temperature $kT=\Delta$ (where k is Boltzmann's constant). For the following relative values of the tunneling parameters: (A) $\mu\gg\mu,\nu$; (B) $\eta=\nu\gg\mu$; (C) $\nu\gg\eta,\mu$.

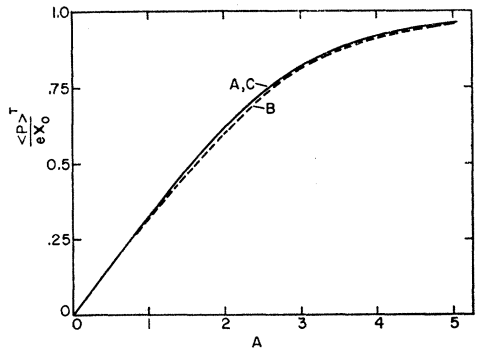

FIG. 15. Thermal average of the XY_6 system's dipole moment $\langle p\rangle^T$ in units of ex_0 as a function of a field applied in the [100] direction, at a temperature $kT=\Delta$ (where k is Boltzmann's constant). For the following relative values of the tunneling parameters: (A) $\eta\gg\mu$; (B) $\eta=\nu\gg\mu$; (C) $\nu\gg\eta,\mu$.

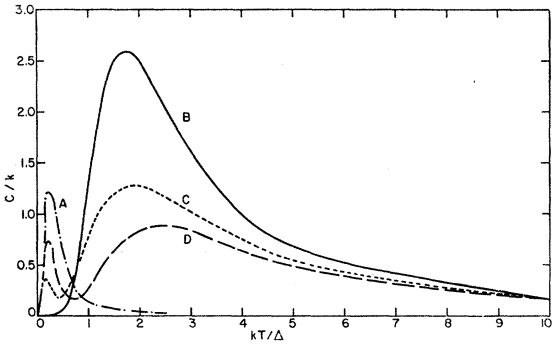

FIG. 16. The specific heat C of the XY_6 system under the influence of an electric field in units of k (Boltzmann's constant), as a function of kT/Δ. For the following electric fields $[A=E_{\rm loc}(ex_0)/\Delta]$: (A) $A=0.0$; (B) $A=5.0$ in the [100] direction; (C) $A=5.0$ in the [110] direction; (D) $A=5.0$ in the [111] direction.

will be possible with the help of Table II to obtain x_0 in a form independent of the tunneling parameters η, μ, ν, and σ by experimentally applying a saturating electric field to the impurity. Once x_0 has been obtained, $E_{\rm loc}$ can be obtained in terms of the applied field by making measurements in the weak-field region.

Figure 16 shows the field-dependent specific-heat anomaly for the XY_6 system. The features are similar to the XY_8 discussed in Sec. II.

APPENDIX IV: STRESS FIELD

The group-theoretic classification of the stress-split levels and the selection rules for allowed electric-dipole transitions for the XY_6 model are shown in Fig. 17 for special symmetry directions.

The irreducible elements of the perturbation $h_\mu(\Gamma^\nu)$ are listed below:

$$h(A_{1g})=\tfrac{1}{3}\sum_{i\neq 0}\left(x_i\frac{\partial}{\partial x_i}+y_i\frac{\partial}{\partial y_i}+z_i\frac{\partial}{\partial z_i}\right)V,\quad h_1(E_g)=\tfrac{1}{6}\sum_{i\neq 0}\left(2z_i\frac{\partial}{\partial z_i}-x_i\frac{\partial}{\partial x_i}-y_i\frac{\partial}{\partial y_i}\right)V,\quad h_2(E_g)=\tfrac{1}{2}\sum_{i\neq 0}\left(x_i\frac{\partial}{\partial x_i}-y_i\frac{\partial}{\partial y_i}\right)V,$$

$$h_1(T_{2g})=\tfrac{1}{2}\sum_{i\neq 0}\left(y_i\frac{\partial}{\partial z_i}+z_i\frac{\partial}{\partial y^i}\right)V,\quad h_2(T_{2g})=\tfrac{1}{2}\sum_{i\neq 0}\left(x_i\frac{\partial}{\partial z_i}+z_i\frac{\partial}{\partial x_i}\right)V,\quad h_3(T_{2g})=\tfrac{1}{2}\sum_{i\neq 0}\left(y_i\frac{\partial}{\partial x_i}+x_i\frac{\partial}{\partial y_i}\right)V,\tag{A4.1}$$

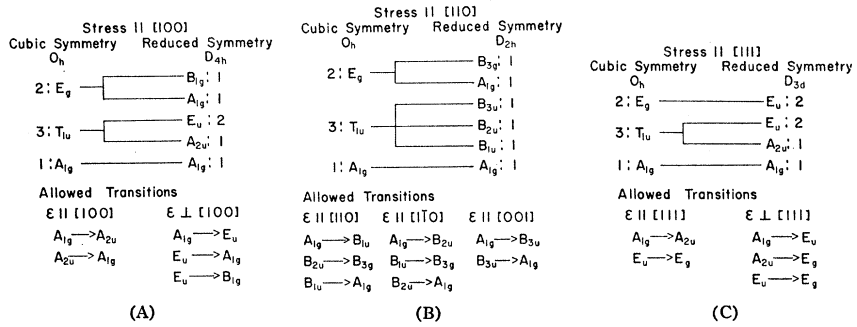

FIG. 17. Group-theoretic classification and allowed electric-dipole transitions for the stress-induced splittings of the XY_6 system, with the stress in the following directions: (A) stress ∥[100]; (B) stress ∥[110]; (C) stress ∥[111].

where the sums are over the lattice equilibrium sites and V is the impurity multi-well potential expressed now as an explicit function of all its neighbor coordinates.

The form of the elements in the expansion of $\langle\psi_p|H'|\psi_q\rangle$ for the T_{1u} state are, for both the XY_8 and XY_6,

$$\langle\psi_p|H'|\psi_q\rangle=\sum_{\mu\nu}H_\mu(\Gamma^\nu)(a_\mu(\Gamma^\nu))_{pq},$$

$$\begin{aligned}
&H(A_{1g})=\tfrac{1}{3}[\langle\psi_x|h(A_{1g})|\psi_x\rangle+\langle\psi_y|h(A_{1g})|\psi_y\rangle+\langle\psi_z|h(A_{1g})|\psi_z\rangle]e(A_{1g}),\\
&H_1(E_g)=\tfrac{1}{6}[2\langle\psi_z|h_1(E_g)|\psi_z\rangle-\langle\psi_x|h_1(E_g)|\psi_x\rangle-\langle\psi_y|h_1(E_g)|\psi_y\rangle]e_1(E_g),\\
&H_2(E_g)=\tfrac{1}{2}[\langle\psi_x|h_2(E_g)|\psi_x\rangle-\langle\psi_y|h_2(E_g)|\psi_y\rangle]e_2(E_g),\\
&H_1(T_{2g})=\langle\psi_y|h_1(T_{2g})|\psi_z\rangle e_1(T_{2g}),\\
&H_2(T_{2g})=\langle\psi_x|h_2(T_{2g})|\psi_z\rangle e_2(T_{2g}),\\
&H_3(T_{2g})=\langle\psi_x|h_3(T_{2g})|\psi_y\rangle e_3(T_{2g}),
\end{aligned}\tag{A4.2}$$

$$a(A_{1g})=\begin{bmatrix}1&0&0\\0&1&0\\0&0&1\end{bmatrix},\quad a_1(E_g)=\begin{bmatrix}-1&0&0\\0&-1&0\\0&0&2\end{bmatrix},\quad a_2(E_g)=\begin{bmatrix}1&0&0\\0&-1&0\\0&0&0\end{bmatrix},$$

$$a_1(T_{2g})=\begin{bmatrix}0&0&0\\0&0&1\\0&1&0\end{bmatrix},\quad a_2(T_{2g})=\begin{bmatrix}0&0&1\\0&0&0\\1&0&0\end{bmatrix},\quad a_3(T_{2g})=\begin{bmatrix}0&1&0\\1&0&0\\0&0&0\end{bmatrix}.$$

The coefficients A, B, and C for the other transitions are as follows. $T_{1u}\rightarrow T_{2g}(XY_8)$:

$$\begin{aligned}
&A=A(T_{2g})-A(T_{1u})=\langle\psi_{yx}(T_{2g})|h(A_{1g})|\psi_{yx}(T_{2g})\rangle-\langle\psi_z(T_{1u})|h(A_{1g})|\psi_z(T_{1u})\rangle,\\
&B=-\tfrac{1}{2}[B(T_{2g})-B(T_{1u})]=[\langle\psi_{xy}|h_1(E_g)|\psi_{xy}\rangle-\langle\psi_z|h_1(E_g)|\psi_z\rangle](-\tfrac{1}{2}),\\
&C=-\tfrac{1}{2}[C(T_{2g})-C(T_{1u})]=-\tfrac{1}{2}[\langle\psi_{yz}|h_3(T_{2g})|\psi_{xz}\rangle-\langle\psi_x|h_3(T_{2g})|\psi_y\rangle].
\end{aligned}\tag{A4.3}$$

For the $T_{2g}\rightarrow A_{2u}$ transition, XY_8, the equations for the [100] and [001] directions must be interchanged as well as interchanging the equations for the [110] and [011] directions.

$$\begin{aligned}
&A=A(A_{2u})-A(T_{2g})=\langle\psi(A_{2u})|h(A_{1g})|\psi(A_{2u})\rangle-\langle\psi_{xy}(T_{2g})|h(A_{1g})|\psi_{xy}(T_{2g})\rangle,\\
&B=-B(T_{2g})=-\langle\psi_{xy}(T_{2g})|h_1(E_g)|\psi_{xy}(T_{2g})\rangle,\\
&C=-C(T_{2g})=-\langle\psi_{yz}(T_{2g})|h_3(T_{2g})|\psi_{xz}(T_{2g})\rangle.
\end{aligned}\tag{A4.4}$$

The $A_{1g}\rightarrow T_{1u}$ transition for XY_6 yields the same result as XY_8. The $T_{1u}\rightarrow E_g$ transition for XY_6 yields:

$$\begin{aligned}
&A=A(E_g)-A(T_{1u})=\langle\psi_2(E_g)|h(A_{1g})|\psi_2(E_g)\rangle-\langle\psi_z(T_{1u})|h(A_{1g})|\psi_z(T_{1u})\rangle,\\
&B=B(E_g)-B(T_{1u})=\langle\psi_1(E_g)|h_1(E_g)|\psi_1(E_g)\rangle-\langle\psi_z(T_{1u})|h_1(E_g)|\psi_z(T_{1u})\rangle,\\
&C=+\tfrac{1}{2}C(T_{1u})=+\tfrac{1}{2}\langle\psi_x(T_{1u})|h_3(T_{2g})|\psi_y(T_{1u})\rangle.
\end{aligned}\tag{A4.5}$$